Available online at www.sciencedirect.com

SCIENCE DIRECT®

Surface Science 600 (2006) 219–228

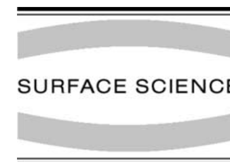

www.elsevier.com/locate/susc

Correlation between local hysteresis and crystallite orientation in PZT thin films deposited on Si and MgO substrates

R. Desfeux [a,*], C. Legrand [a], A. Da Costa [a], D. Chateigner [b], R. Bouregba [b], G. Poullain [b]

[a] *Laboratoire de Physico-Chimie des Interfaces et Applications, CNRS-FRE 2485, Université d'Artois, Faculté des Sciences Jean Perrin, Rue Jean Souvraz, SP 18, 62307 Lens Cedex, France*

[b] *Laboratoire de Cristallographie et Sciences des Matériaux, CNRS-UMR 6508, CRISMAT-ENSICAEN, 6 Boulevard du Maréchal Juin, 14050 Caen Cedex, France*

Received 2 May 2005; accepted for publication 16 September 2005
Available online 21 November 2005

Abstract

(001)-Oriented tetragonal ferroelectric $PbZr_{0.53}Ti_{0.47}O_3$ (PZT) thin films (90 nm of thickness) have been grown on $TiO_x/Pt/TiO_2/SiO_2/Si$ and $TiO_x/Pt/MgO$ substrates. The existence of (100)-oriented crystallites in the *c*-axis matrix of the (001)-oriented films has been evidenced by using four circles X-ray diffraction. Depending on the substrate, the ratio of the lattice parameters c/a was found to be 1.02 (Si) and 1.07 (MgO) and this was correlated with the coercive field values. Local piezoelectric hysteresis loops produced by atomic force microscopy have been taken with profit to characterize the switching properties of the ferroelectric domains at the scale of individual crystallites. In each case, (100)-oriented crystallites require much higher voltage than (001)-oriented crystallites for switching. These results are explained by taking into account the strain imposed by the substrate in the film. We conclude that piezoelectric hysteresis loops produced by atomic force microscopy provide very rich information for addressing the local switching property of individual crystallites in PZT thin films.
© 2005 Elsevier B.V. All rights reserved.

Keywords: Ferroelectric films; Four-circle diffractometry; Atomic force microscopy; Local piezoelectric hysteresis loops; Thin film structures; Surface structure, morphology, roughness, and topography; Piezoelectric effect

* Corresponding author.
E-mail address: desfeux@univ-artois.fr (R. Desfeux).

0039-6028/$ - see front matter © 2005 Elsevier B.V. All rights reserved.
doi:10.1016/j.susc.2005.09.053

1. Introduction

$PbZr_xTi_{1-x}O_3$ (PZT) thin films are currently being investigated for applications due to their remarkable piezoelectric, pyroelectric and ferroelectric properties [1–9]. By taking advantage of the anisotropic properties of such oxides, different groups have shown that it is possible to adjust the electrical characteristics of the films (dielectric constant ε_r, remanent polarization P_r, coercive field E_c...) by controlling their crystallographic orientation. In this way, highly (1 0 0)-, (1 1 1)- and (0 0 1)-heteroepitaxial or fibre-like textures have been achieved in thin films in the last few years [8,10–15]. With the high degree of miniaturization, one of the challenges is to reduce the lateral sizes of the film-unit required for the applications, while keeping the properties of the material. Ferroelectricity represents a cooperative phenomenon that relies on the interaction of neighbouring permanent electric dipoles in crystal lattice [3]. Then, a particular point to explore is how behaves the material from a ferroelectric point of view when reducing the probed area under measurement, it means when going from the macroscopic scale (by using large area electrode for measurement) to the nanoscopic scale. One should keep in mind that there is a size limit below which ferroelectricity vanishes and that the existence of defects such as grain boundaries in the film can play an important role on the measured electrical properties [16]. Disoriented crystallographic domains can also be present in the highly oriented matrix of the film which may modify locally the electric properties of the oxide.

In a previous paper, we demonstrated that the threshold voltages required to switch the ferroelectric domains of highly oriented PZT films at the microscopic scale were fully correlated to the coercive values determined at the macroscopic scale by using large electrodes (250 μm × 250 μm) [5]. The microscopic results were obtained by means of electrostatic force microscopy (EFM). Unfortunately, no local electrical data (at the nanoscale level) could be given by this technique mainly due to the resolution range (about 1 μm). In this paper, we demonstrate that atomic force microscopy can provide quantitative electrical information at the nanoscale level by considering local piezoelectric hysteresis loops. By correlating structural data obtained by quantitative texture analysis using four-circle diffractometry and the values of coercive voltages measured on local hysteresis loops produced by atomic force microscopy when mapping the surface of the films, we relate the switching properties to the crystallite orientation of (0 0 1)-oriented PZT films grown on two kinds of substrates, $TiO_x/Pt/TiO_2/SiO_2/Si$ and $TiO_x/Pt/MgO$.

2. Experimental procedure

2.1. Thin film deposition

$PbZr_{0.53}Ti_{0.47}O_3$ (PZT) thin films have been grown by radio-frequency magnetron sputtering on two kinds of substrates (i) Si(1 0 0) wafers with 400 nm thermally grown silicon dioxide and (ii) MgO(2 0 0) single crystals. On SiO_2/Si(1 0 0), a TiO_2 thin layer (20 nm) was first deposited in order to promote the adhesion of the (1 1 1)-oriented platinum (Pt) bottom electrode (100 nm). The TiO_2 layer was grown at 450 °C under a mixed atmosphere of argon (95%) and oxygen (5%) while the platinum layer was deposited in a pure argon atmosphere. On MgO(2 0 0) substrates, the platinum bottom electrode (100 nm) was directly deposited on the substrate at 500 °C in argon. In this case, the platinum was (2 0 0)-oriented. In order to control the orientation of the PZT film, a thin layer of TiO_x (2 nm) was next deposited on the $Pt/TiO_2/SiO_2/Si$ and Pt/MgO samples. For this upper layer, the temperature was adjusted to 500 °C and the atmosphere was pure argon. Finally, the PZT thin films were deposited on TiO_x at 500 °C under an atmosphere of 20% of oxygen and 80% of argon. Three Ti, Zr and Pb metallic targets and a spinning substrate holder were used. The total pressure was kept at 0.4 Pa during the PZT sputtering. To eliminate extrinsic factors during the PZT growth, the films were deposited in the same run on the two $TiO_x/Pt/TiO_2/SiO_2/Si$ and TiO_x/Pt/MgO samples. The thickness of the PZT films is 90 nm.

2.2. Structural characterization

X-ray diffraction analysis was operated using a 4-circle texture goniometer equipped with a Curved Position Sensitive (CPS 120) detector from INEL and with the monochromatised Cu Kα radiation. Such a setup provides the full diffraction diagram at once for each tilt and azimuth (χ, φ) sample orientation [17,18]. We measured the (001)-oriented samples using an incident beam at $\omega = 10.75°$ centred on the {100/001} reflection. The scan was operated in the 0–10° χ-range and 0–360° φ-range with steps of 1° for both angles. Such a scan is able to check for the film planes parallel to the sample plane or slightly tilted relative to this plane (up to 10°). A Rietveld fitting procedure over all the diagrams measured for all the sample orientations was carried out in order to deconvolute the (001) and (100) contributions and extract the corresponding pole figures [18].

X-ray $\theta/2\theta$ diffraction spectra shown in the paper have been performed using a Rigaku Miniflex + diffractometer (filtered Cu Kα_1 radiation). The relatively high background is attributed to a signature of the anticathode spectrum.

2.3. Surface morphology and electrical characterizations

The surface morphology and electrical investigations were carried out in air at room temperature by using a Veeco Nanoscope IIIa scanning force microscope. For surface morphology characterizations, atomic force microscopy measurements were performed in the contact mode with Si ultralever tips, using a small repulsion force. For electrical investigations, local piezoelectric hysteresis loops were recorded for the measurement of the coercive voltage V_c. Coercive voltage corresponds to the voltage required to put the poled area of the sample localized beneath the tip to the zero-polarization state. The experiments were carried out by considering the so-called "in field" mode which presents the particular characteristic to be very close to the one used for "macroscopic" hysteresis loops recording [19–21]. In brief, this mode consists in applying a continuous bias voltage between the tip and the ground platinum bottom electrode together with an alternative voltage of the form $V = V_{ac}\cos(2\pi ft)$ which induces the electromechanical vibration of the sample. The signal generated by the piezoelectric vibration (PFM signal) and fed from the photodetector to a lock-in amplifier is of the form $A\cos\varphi$. The amplitude A of the first harmonic signal of the vibration is related to the piezoelectric coefficients of the sample, while the phase shift φ between the alternative reference voltage and the first harmonic signal depends on the direction of the polarization in the film [22]. Our main goal being to study the switching properties of the films, only the local piezoelectric hysteresis loops recorded in phase will be shown in this paper. For our experiments, the DC voltage was gradually increased from −10 V to +10 V then decreased from +10 V down to −10 V within a period of 100 s. The voltage step was adjusted to $\delta V = 0.4$ V. A total of 500 measurement points were recorded for each hysteresis loop. Platinum/iridium coated silicon tip with a stiffness of 1.2–5.5 N/m were used. The frequency of the applied AC voltage was adjusted to 2 kHz with a driving voltage of 0.5–1.5 V. In this work, the coercive voltage V_c was calculated using $V_c = [V_c(+) + |V_c(-)|]/2$ where $V_c(+)$ and $V_c(-)$ were the coercive voltages extracted from the local piezoelectric hysteresis loops for the positive and negative poling, respectively.

3. Results and discussion

3.1. X-ray $\theta/2\theta$ diffraction measurements

Fig. 1 is a plot of the X-ray $\theta/2\theta$ diffraction spectra of PZT films grown on TiO_x/Pt/TiO_2/SiO_2/Si and TiO_x/Pt/MgO substrates. Depending on the substrate, Si or MgO, the spectra evidence the existence of the (111) reflection or (200) reflection of the platinum. Also, for the two substrates, the spectra exhibit mainly the (001) and (002) reflections of the PZT perovskite. However, in the case of the film grown on TiO_x/Pt/TiO_2/SiO_2/Si, (100) and (200) reflections can be distinguished. This reveals that the films contain a

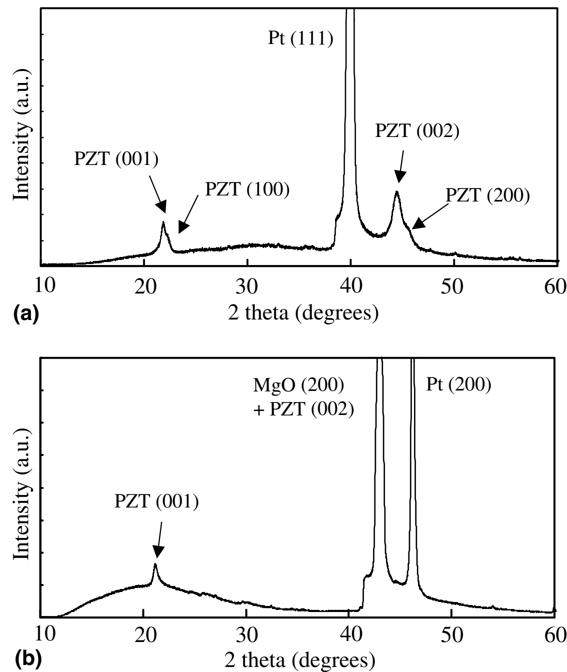

Fig. 1. X-ray $\theta/2\theta$ diffraction spectra of $PbZr_{0.53}Ti_{0.47}O_3$ films (90 nm of thickness) grown on (a) $TiO_x/Pt/TiO_2/SiO_2/Si$ and (b) $TiO_x/Pt/MgO$ substrates.

non-negligible volume fraction of *a*-axis oriented grains. The lattice parameters of the PZT films are $a = 0.40555(4)$ nm and $c = 0.4127(1)$ nm on $TiO_x/Pt/TiO_2/SiO_2/Si$ and $a = 0.3935(4)$ nm and $c = 0.41971(4)$ nm on $TiO_x/Pt/MgO$, as refined using the combined analysis in the quantitative texture analysis step [18].

3.2. Atomic force microscopy measurements

Fig. 2 shows AFM images recorded at the surface of the PZT films grown on the two kinds of substrates. The images have been recorded over scan regions of $1 \times 1\ \mu m^2$. For the two types of samples, the surface morphology is quite similar with the existence of a dense granular-like surface. On $TiO_x/Pt/TiO_2/SiO_2/Si$ substrates, the grains are quite round with a mean diameter of about 80 nm. On $TiO_x/Pt/MgO$, the grains appear more interconnected to each other and their diameter is about 150 nm. The root mean square (R_{ms}) values of the roughness for scan areas of $5 \times 5\ \mu m^2$ are

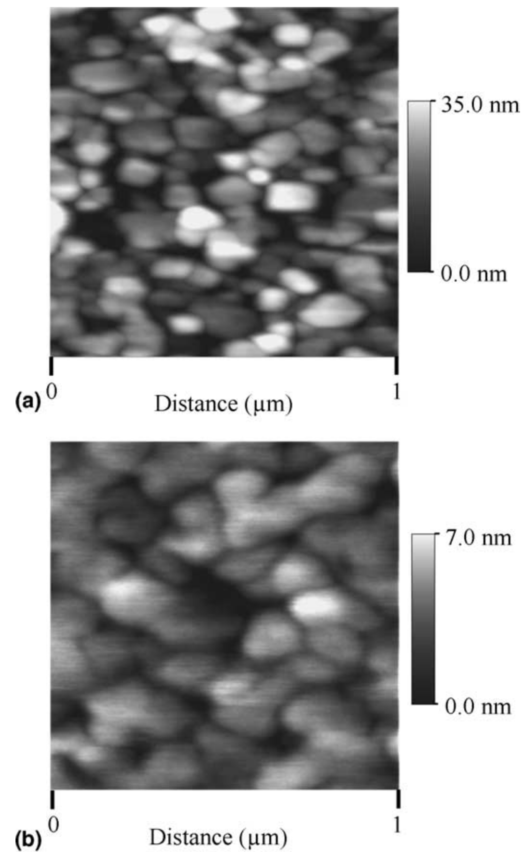

Fig. 2. AFM images of the (001)-oriented ferroelectric PZT films grown on (a) $TiO_x/Pt/TiO_2/SiO_2/Si$ and (b) $TiO_x/Pt/MgO$ substrates. The scan sizes are $1\ \mu m \times 1\ \mu m$.

7.8 nm and 2.6 nm on $TiO_x/Pt/TiO_2/SiO_2/Si$ and $TiO_x/Pt/MgO$, respectively.

3.3. Electrical measurements at the macroscale level

In order to investigate the ferroelectric properties of the two kinds of films, *D–E* hysteresis loops were measured at the macroscopic scale level using a conventional Sawyer-Tower circuit with a 200 Hz sine wave. Large area Pt top electrodes ($250\ \mu m \times 250\ \mu m$ in size) were deposited by lift-off on the samples, this means that many crystallites and grain boundaries were taken into account for the measurement. Fig. 3 shows the hysteresis loop recorded for the 90 nm thick (001)-oriented

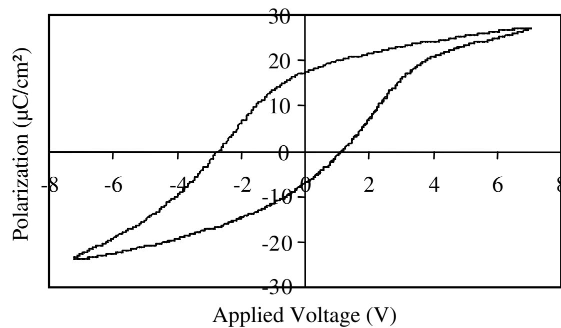

Fig. 3. *D–E* hysteresis loop of the 90 nm thick PZT film grown on TiO_x/Pt/MgO substrate. A large electrode (250 µm × 250 µm) deposited on the top of the film was used for measurement.

PZT film deposited on TiO_x/Pt/MgO. An average coercive voltage of 1.9 V (210 kV/cm) is measured for this film. The shift of the loop may be attributed to an internal electric field which may result from the difference between top and bottom platinum electrode preparation. On the other hand, no macroscopic hysteresis loop could be obtained for the film deposited on TiO_x/Pt/Ti/SiO_2/Si due to important current leakage. This was attributed to the large value of the R_{ms} root mean-square roughness for this 90 nm thick film (R_{ms} = 7.8 nm). As reported by other groups for PZT ferroelectric films, the coercive voltage is decreasing with the increase of the film thickness [23,24]. For such a 90 nm thick (001)-oriented PZT film grown on TiO_x/Pt/Ti/SiO_2/Si, a coercive voltage value of around 1.1 V is expected as deduced from measurements on thicker films.

3.4. Local piezoelectric hysteresis loops at the nanoscale level and four-circle X-ray diffraction measurements

In order to get information about the switching properties of the films at the nanoscale level, inves-

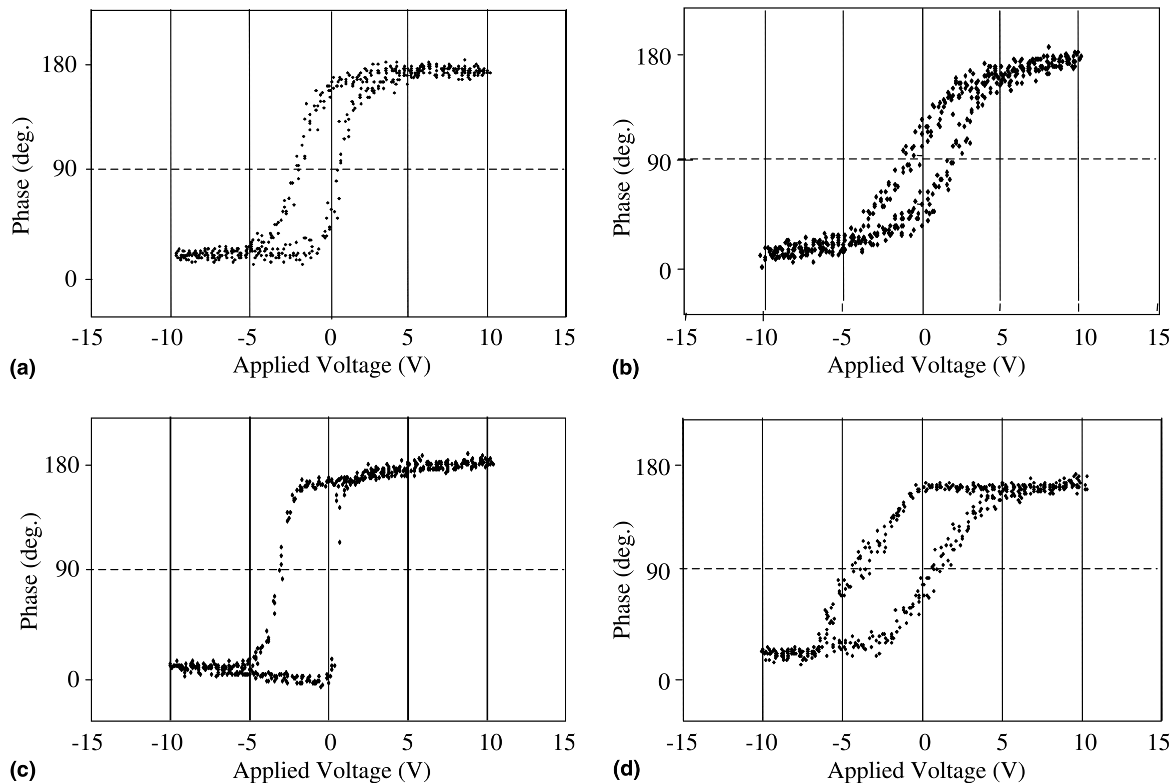

Fig. 4. Typical local piezoelectric hysteresis loops recorded at the surface of crystallites of the films grown on (a) and (b) TiO_x/Pt/TiO_2/SiO_2/Si and (c) and (d) TiO_x/Pt/MgO substrates.

tigations were carried out by carefully positioning the tip of an AFM at the center of crystallites observed at the surface of the films. The diameter of the apex of the tip is $\leqslant$30 nm. Fig. 4 shows typical local piezoelectric hysteresis loops recorded for each substrate. As a first observation, asymmetry in the switching parameters (coercive voltages) is evidenced on the hysteresis loops. This asymmetry was found to be dependent on the crystallite investigated. This behavior has already been observed by different groups [7,9,25,26]. Commonly, this asymmetry was either attributed to an internal built-in electric field at the bottom interface or/and to the tip/film/electrode heterostructure which brings its own asymmetry. While the asymmetry depends on the crystallite measured, we chose to give the V_c coercive voltage values by considering the average of the coercive values measuring from the positive and negative poling, $V_c(+)$ and $V_c(-)$, respectively. As a second observation, it should be noted that the V_c value was strongly dependent on the crystallite studied. In order to get a sight about the distribution of V_c for the two kinds of oriented films, histograms representing the probability of hysteresis loops versus the V_c-range are shown in Fig. 5 for our two samples. V_c ranges were discretised in 0.1 V intervals and the amount of grains corresponding to each range counted. Fifty hysteresis loops were measured for each sample.

Quantitatively, there are two components of a bimodal distribution of V_c around 0.8 V and 1.3 V for the film deposited on $Pt/TiO_2/SiO_2/Si$ substrate (Fig. 5(a)). This is attributed to the two (1 0 0) and (0 0 1) grain orientations in the film as detected by $\theta/2\theta$ X-ray measurements. In this case, we observe that around 70% of the coercive voltage values are included between 0.7 V and 0.9 V leading to the average value of 0.8 V, and 30% are spread between 0.9 V and 2 V. Quantitative texture measurements allowed the reconstruction of the two {1 0 0} and {0 0 1} pole figures (Fig. 6), representative of the *a*- and *c*-axes distribution around the normal to the sample plane,

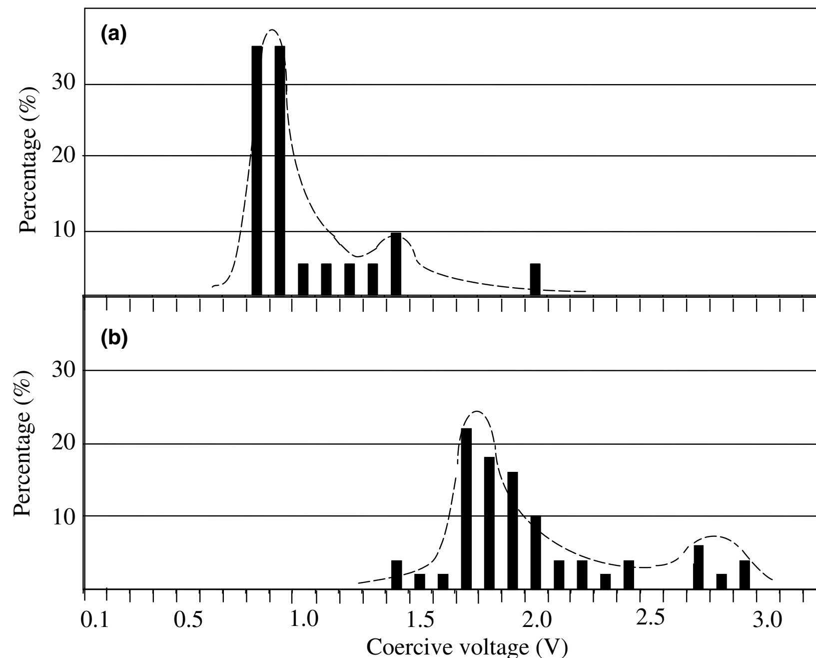

Fig. 5. Histograms giving the percentage of hysteresis loops versus the coercive voltage for 90 nm thick PZT films deposited on (a) $TiO_x/Pt/TiO_2/SiO_2/Si$ and (b) $TiO_x/Pt/MgO$ substrates. (Range of coercive voltages: 0.1 for [0–0.1 V[, 0.2 for [0.1–0.2 V[, ... , 0.5 for [0.4–0.5 V[, ... , 1.0 for [0.9–1.0 V[, ... , 3.0 for [2.9–3.0 V[, ...).

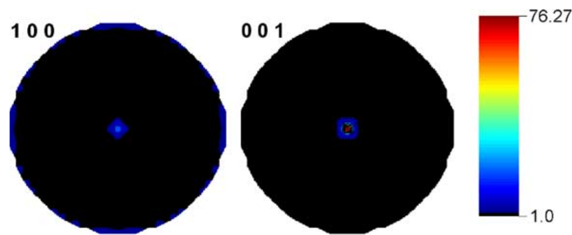

Fig. 6. {001} and {100} pole figures recalculated after quantitative texture analysis has been performed, for the film deposited on Si. Values on the scale bar are in multiple of a random distribution, linear density scale, equal area projection. Integration of the figures over all the measured points gives 70% of the volume oriented with *c*-axes and 30% with *a*-axes perpendicular to the film plane, respectively.

respectively. Integration over the {001} and {100} poles confirm that around 70% and 30% of the sample volume is oriented with *c*- and *a*-axes perpendicular to the sample plane, respectively. Our interpretation is then that the 70% of (001)-oriented grains as determined by X-ray diffraction corresponds to the 70% of the grains with low coercive field measured by AFM. The peculiar value of 0.8 V is the most favored for the switching process in the case of (001)-oriented grains on TiO_x/Pt/TiO_2/SiO_2/Si substrates. Larger V_c-values, between 0.9 V and 2 V, may correspond to the (100)-oriented grains. Indeed for this orientation, the polarization axis lays in the plane of the substrate at the virgin state before the application of the external voltage. Then, one needs larger fields to invert the $\langle a \rangle$ and $\langle c \rangle$ axes of the lattice. This may lead to larger coercive field than in the case of pure (001) orientation for which only a polarization reversal is needed. The large range of coercive field values may be assigned to disorientation of some crystallites with respect to the sample plane in such grains or to different localized strains imposed by the substrate.

For the PZT film deposited on TiO_x/Pt/MgO substrate which is highly (001)-oriented as observed from $\theta/2\theta$ measurements, we surprisingly also observed two average V_c-values around $V_{c1} = 1.7$ V and $V_{c2} = 2.7$ V (Fig. 5(b)). Fig. 4(c) and (d) shows that as in the case of the silicon substrate, there are two different shapes for the hysteresis loops. 88% of the V_c-values are observed between 1.3 V and 2.4 V while 12% remained in a second distribution component between 2.6 V and 2.9 V. This second kind of hysteresis loop was characterized by a different slope. In order to get a better insight on the bimodal distribution, the crystallographic structure and texture of the (001)-oriented film on MgO substrate were measured. Fig. 7 shows typical 2θ diagrams measured at no sample tilt (Fig. 7(a)) and with a 3° tilt (Fig. 7(b)) in the (001/100) reflection range. The strong 001 peak (Fig. 7(a)) is asymmetric towards the large θ angles. This asymmetry reveals the presence of compositional distributions in this film. Such compositional variations may give rise to small volume fraction of the material with different ferroelectric properties and then different

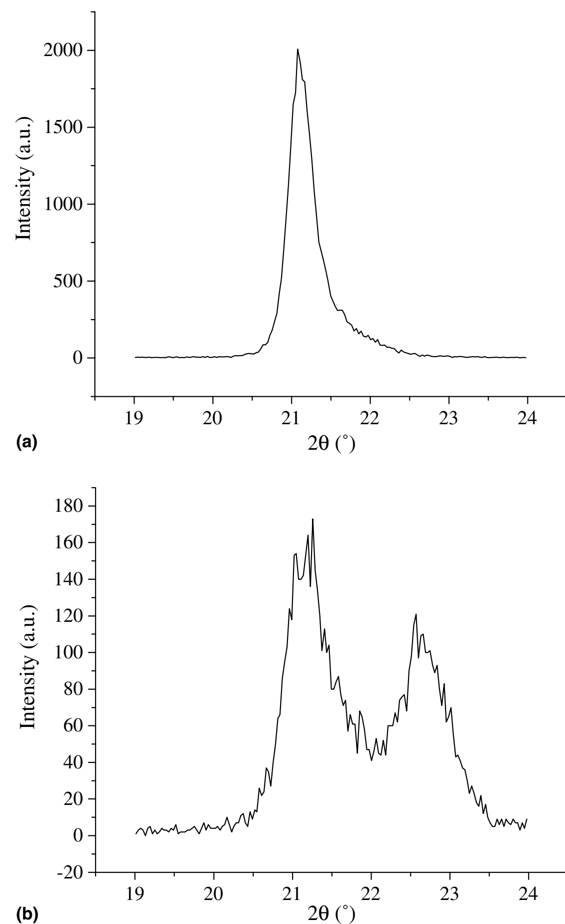

Fig. 7. 2θ diagrams measured at $\chi = 0°$ (a) and $\chi = 3°$ (b) for the film grown on TiO_x/Pt/MgO substrate.

coercive voltages under the AFM tip. This may explain partly the broadening of the V_c values at the right hand side of the maximum values in Fig. 5(a) and (b).

At larger tilt angles (Fig. 7(b)), the 001 peak decreases rapidly being of comparable intensity to a 100 contribution which appears around 3° tilts. Fig. 8 represents the evolution of the {001} and {100} distribution densities in function of the tilt angle χ. On this diagram, all intensities at every φ position have been summed for each χ, and then normalized into distribution densities using the direct integration approach [27]. The film exhibits a very high level of orientations for both orientation components with a maximum density at $\chi = 0°$ around 1300 m.r.d. (on such a diagram a perfectly randomly oriented powder would take the constant value of 1 m.r.d.). The most interesting feature of this graph is that it shows a non-negligible amount of crystallites with (100) planes nearly parallel to the sample plane (which in fact points around $\chi = 2.5°$). The existence of such slightly inclined (100) grains was reported before [28–31]. The disorientation angle of the (100) grains was shown to follow the expression $[2\tan^{-1}(c/a)] - 90°$ [31]. In our case where $c/a = 1.07$, this should lead to an angle of 3.9° for a fully relaxed thin film. As we measured an angle of 2.5°, this implies that some stress is remaining in the film. A precise quantitative determination of the concerned volume fraction of such a texture component is not possible at the present time because it would need a full orientation distribution function determination, which is not available for measuring grids of $1° \times 1°$ at the present time. However, the direct integration approach allows us to determine an upper limit for this volume fraction of around 10% by integration of the distribution density curves. This would be more than enough to produce the second hysteresis contribution V_{c2} of our film.

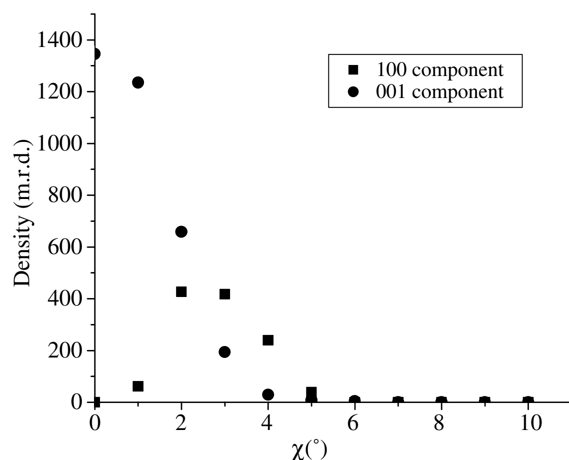

Fig. 8. {001} and {100} distribution density plot of the film deposited on $TiO_x/Pt/MgO$ substrate.

The assignment of V_{c2} hysteresis cycles to the (100)-oriented crystallites may also explain why in mainly (001)-oriented films the V_{c2}-linked hysteresis cycles are more inclined than the V_{c1}'s. Indeed, as proposed previously in this paper, in the case of (100)-oriented tetragonal crystallites, the lattice has to be distorted when the external field is applied in such a way that the polar axis ([001] direction) becomes perpendicular to the plane of the substrate. In the case of PZT films on $TiO_x/Pt/TiO_2/SiO_2/Si$ substrates, the c/a ratio is quite low (1.02) and the external voltage needed to reorient the dipoles is also reasonably low. But in the case of $TiO_x/Pt/MgO$, due to different strain imposed by the substrate, c/a is now large (1.07) and consequently a large external voltage is needed for the polarization reversal. As the field is set in the opposite direction, the reorientation of the dipoles has to overcome the strains which were responsible for the (100) orientation of these crystallites. This is difficult and leads to a very progressive reversal of this kind of dipoles, implying a high coercive voltage and an inclined hysteresis loop (Fig. 4(d)). On the other hand, when the polarization reversal concerned crystallites which were "naturally" (001) oriented (Fig. 4(c)), the sole energy needed to reverse the dipoles is to rotate them by 180°. This arises when the applied field reaches a given threshold energy. Note that this threshold energy is an increasing function of the tetragonality of the lattice. Indeed, c/a is an increasing function of the ratio Ti/Zr, and it is well known that the coercive field is also an increasing function of the ratio Ti/Zr [32]. Hence in the case of (001) oriented grains, a very abrupt reversal of the dipoles is expected when the applied field

exceeds the threshold field, and consequently a more "square like" shape of the hysteresis loop is obtained (Fig. 4c). Now, in the case of the crystallites with (1 0 0) orientation on $TiO_x/Pt/TiO_2/SiO_2/Si$ substrate, the X-ray analysis showed that the tetragonality of the lattice is much lower than for the $TiO_x/Pt/MgO$ substrate (1.02 instead of 1.07). This could explain the lower coercive measured voltages (c/a is much lower than in the case of the $TiO_x/Pt/MgO$ substrate), with an intermediate slope, because the applied field has still to overcome the strains needed to distort the lattice and exchange *a*- and *c*-axes during the polarization process.

4. Conclusion

Local piezoelectric hysteresis loops produced by atomic force microscopy have been used to determine the coercive voltage of oriented PZT thin films deposited on $TiO_x/Pt/TiO_2/SiO_2/Si$ and $TiO_x/Pt/MgO$ substrates. These different substrates are directly responsible for a difference in the c/a ratio of the PZT thin films, as evidenced by the fact that the films were prepared in the same run. The c/a ratios were 1.02 and 1.07 for $TiO_x/Pt/TiO_2/SiO_2/Si$ and $TiO_x/Pt/MgO$ substrates, respectively. The local piezoelectric loops recorded on individual crystallites showed a bimodal coercive field values which were attributed to the presence of two different grain orientations, namely (1 0 0) and (0 0 1). For each substrate, (0 0 1)-oriented grains exhibited lower coercive voltage than (1 0 0) ones. This was attributed to the different orientation of the polar axis. The influence of the c/a ratio is also evidenced by comparing grains having the same orientation on both substrates. Large coercive fields are obtained when the c/a ratio is high, as expected. All these results demonstrate that the local piezoelectric hysteresis loops performed by atomic force microscopy are very powerful for addressing the local switching properties of such kind of films. We have shown that the value of the coercive voltage could be related to the crystallographic orientation of the crystallite at the nanoscale level. On the other hand, for films grown on $TiO_x/Pt/TiO_2/SiO_2/Si$, we have shown that data about coercive voltages could be measured at the nanoscale level while no information could be given at the macroscopic scale level, using large area electrodes, due to current leakages.

Acknowledgements

The authors of LPCIA would like to thank L. Maës for technical support. D. Chateigner greatly acknowledges the "Région Basse-Normandie" for partial financing of the Quantitative Texture Diffractometer.

References

[1] C. Ahn, K. Rabe, J.M. Triscone, Science 303 (2004) 488.
[2] R. Bouregba, B. Vilquin, G. Le Rhun, G. Poullain, B. Domenges, Rev. Sci. Instrum. 74 (2003) 4429.
[3] X.Y. Zhang, X. Zhao, C.W. Lai, J. Wang, X.G. Tang, J.Y. Dai, Appl. Phys. Lett. 85 (2004) 4190.
[4] A.K. Sarin Kumar, P. Paruch, J.M. Triscone, W. Daniau, S. Ballandras, L. Pellegrino, D. Marré, T. Tybell, Appl. Phys. Lett. 85 (2004) 1757.
[5] R. Desfeux, A. Da Costa, A. Flambard, C. Legrand, D. Tondelier, G. Poullain, R. Bouregba, Appl. Surf. Sci. 228 (2004) 34.
[6] D. Rèmiens, E. Cattan, C. Soyer, T. Haccart, Mater. Sci. Semi. Process. 5 (2003) 123.
[7] V.V. Shvartsman, A.L. Kholkin, N.A. Pertsev, Appl. Phys. Lett. 81 (2002) 3025.
[8] C. Soyer, E. Cattan, D. Rèmiens, M. Guilloux-Viry, J. Appl. Phys. 92 (2002) 1048.
[9] A. Gruverman, A. Kholkin, A. Kingon, H. Tokumoto, Appl. Phys. Lett. 78 (2001) 2751.
[10] R. Bouregba, G. Poullain, B. Vilquin, H. Murray, Mater. Res. Bull. 35 (2000) 1381.
[11] R. Bouregba, G. Poullain, B. Vilquin, H. Murray, Ferroelectrics 256 (2001) 47.
[12] T. Tybell, C.H. Ahn, J.M. Triscone, Appl. Phys. Lett. 72 (1998) 1454.
[13] S-H. Kim, D.-Y. Park, H.-J. Woo, D.-S. Lee, J. Ha, C.S. Hwang, I.-B. Shim, A.I. Kingon, Thin Solid Films 416 (2002) 264.
[14] D. Chateigner, H.-R. Wenk, A. Patel, M. Todd, D.J. Barber, Integr. Ferroelectr. 19 (1998) 121.
[15] N.A. Pertsev, J. Rodriguez Contreras, V.G. Kukhar, B. Hermanns, H. Kohlstedt, R. Waser, Appl. Phys. Lett. 83 (2003) 3356.
[16] J. Junquera, P. Ghosez, Nature 422 (2003) 506.
[17] J. Ricote, D. Chateigner, Bol. Soc. Esp. Ceram. Vidrio 38 (1999) 587.

[18] D. Chateigner (Ed.), Combined analysis: structure-texture-microstructure-phase-stresses-reflectivity analysis by X-ray and neutron diffraction, 2004, p. 143. Available from: <http://www.ecole.ensicaen.fr/~chateign/texture/combined.pdf>.

[19] S. Hong, J. Woo, H. Shin, J.U. Jeon, Y.E. Pak, E. Kim, K. No, J. Appl. Phys. 89 (2001) 1377.

[20] H.Y. Guo, J.B. Xu, I.H. Wilson, Z. Xie, E.Z. Luo, S. Hong, H. Yan, Appl. Phys. Lett. 81 (2002) 715.

[21] B. Gautier, J.R. Duclere, M. Guilloux-Viry, Appl. Surf. Sci. 217 (2003) 108.

[22] S.V. Kalinin, D.A. Bonnell, Phys. Rev. B 65 (2002) 125408.

[23] A.K. Tagantsev, Cz. Pawlaczyk, K. Brooks, N. Setter, Integr. Ferroelectr. 4 (1994) 1.

[24] Y. Sakashita, H. Segawa, K. Tominaga, M. Okada, J. Appl. Phys. 73 (1993) 7857.

[25] S. Dunn, R.W. Whatmore, J. Eur. Ceram. Soc. 22 (2002) 825.

[26] H. Fujisawa, M. Okaniwa, H. Nonomura, M. Shimizu, H. Niu, J. Eur. Ceram. Soc. 24 (2004) 1641.

[27] E. Guilmeau, R. Funahashi, M. Mikami, K. Chong, D. Chateigner, Appl. Phys. Lett. 85 (2004) 1490.

[28] C.M. Foster, Z. Li, M. Buckett, D. Miller, P.M. Baldo, L.E. Rehn, G.R. Bai, D. Guo, H. You, K.L. Merkle, J. Appl. Phys. 78 (1995) 2607.

[29] W.Y. Hsu, R. Raj, Appl. Phys. Lett. 67 (1995) 792.

[30] C.M. Foster, W. Pompe, A.C. Daykin, J.S. Speck, J. Appl. Phys. 79 (1995) 1405.

[31] J.S. Speck, A.C. Daykin, A. Seifert, J. Appl. Phys. 78 (1995) 1696.

[32] C.M. Foster, G.R. Bai, R. Csencsits, J. Vetrone, R. Jammy, L.A. Wills, E. Carr, J. Amano, J. Appl. Phys. 81 (1997) 2349.